JOURNAL OF SOLID STATE CHEMISTRY 88, 261–268 (1990)

Structural Aspects and Mössbauer Resonance Investigation of $Ba_2Fe_2O_5$

M. PARRAS,* L. FOURNES, J-C. GRENIER,[1] M. POUCHARD, M. VALLET,* J. M. CALBET,* AND P. HAGENMULLER

*Laboratoire de Chimie du Solide du CNRS, Université de Bordeaux I, 33 405 Talence Cédex, France; and *Facultad de Ciencias Quimicas, Departamento de Quimica Inorganica, Universidad Complutense, 28040 Madrid, Spain*

Received February 20, 1990

DEDICATED TO J. M. HONIG ON THE OCCASION OF HIS 65TH BIRTHDAY

Barium ferrite $Ba_2Fe_2O_5$ has been studied using various techniques. X-ray diffraction and TEM have shown the phase to crystallize with a monoclinic symmetry, the unit cell being a complex supercell of a cubic perovskite cell. The Mössbauer resonance spectrum exhibits five sextuplets which have been assigned to Fe^{3+} in O_h, T_d, and fivefold coordinated sites. Obviously $Ba_2Fe_2O_5$ does not adopt the brownmillerite structure of homologous calcium (or strontium) ferrite and the oxygen vacancy ordering is more complex.

A recent reinvestigation of the $BaFeO_{3-y}$ system has shown that a transition in the structural stacking occurs in the vicinity of $y = 0.35$ (i.e., with a Fe^{4+}/Fe^{3+} ratio ca $\frac{1}{3}$) (*1*). It has been attributed to the variation of the so-called Goldschmidt tolerance factor which increases with the Fe^{4+} content. For $y < 0.35$, the symmetry is hexagonal of 12H- or 6H-type according to y, while for $y > 0.35$, X-ray diffraction reveals a macroscopic cubic or cubic-related symmetry. HRTEM observations in the composition range $0.35 \lesssim y \lesssim 0.50$ have shown in fact the occurrence of complex microstructures resulting probably from a particular vacancy ordering (*2*). They derive either from an orthorhombic phase with a composition close to $BaFeO_{2.54}$ or from the below-described monoclinic structure of $Ba_2Fe_2O_5$ (*3*).

Until recently $A_2Fe_2O_5$ compounds (A = Ca, Sr, or Ba) were considered as crystallizing with the orthorhombic brownmillerite structure (*4–6*) though the X-ray diffraction data for $Ba_2Fe_2O_5$ were somewhat controversial (*7–9*). In a previous paper (*3*) we have shown using TEM that the true unit cell was actually not of brownmillerite-type but characterized by a large monoclinic unit cell deriving nevertheless from the perovskite one. In addition this compound undergoes a beam-induced structural transition leading to orthorhombic symmetry (*10*). In both varieties the structure does not seem to be directly related to the well-known brownmillerite structure.

The present work is devoted to structural

[1] To whom correspondence should be addressed.

0022-4596/90 $3.00

and physical characterizations of this monoclinic phase especially the Mössbauer spectroscopy. The results are compared to those previously obtained for the homologous calcium and strontium ferrites.

Experimental

$Ba_2Fe_2O_5$ was prepared as previously described (*1*): a stoichiometric mixture of $BaCO_3$ and α-Fe_2O_3 was finely ground, then heated at 1100°C for 24 hr under pure N_2 atmosphere and, finally, slowly cooled under the same conditions ($\simeq$ 20°C/hr). The obtained material was brown and it was analytically shown to be free from Fe^{4+}.

Taking into account the rather complex X-ray diffraction pattern of this compound, a refinement using the Rietveld method has been tentatively carried out starting from powder X-ray diffraction data collected on a Siemens D-500 diffractometer.

In a first step, the space group has been determined. Thus, on the basis of our previously published electron diffraction patterns (*3*), the diffraction reflections are the following:

—(hkl), without condition; —($h0l$), $l = 2n$.[2]

Moreover additional observations have been performed. For instance, Fig. 1 represents the electron diffraction pattern of $Ba_2Fe_2O_5$ along the $[10\bar{2}]_m$ zone axis. Only the $k = 2n$ reflections along the ($0k0$) reciprocal axis are observed.

Therefore, with a monoclinic symmetry, all these diffraction conditions correspond unambiguously to the $P2_1/c$ space group (*11*).

The relation between the monoclinic and cubic perovskite reciprocal cells deduced from the HRTEM observations (*3*) can be expressed as follows:

[2] The a^* and c^* axes should be inverted in the electron diffraction patterns of Ref. (*3*) in order to agree with the international notation.

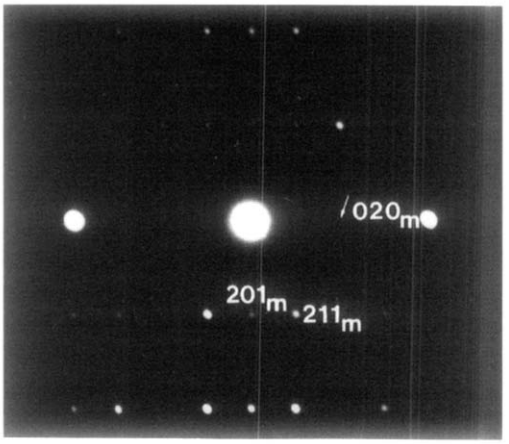

FIG. 1. Electron diffraction pattern of $Ba_2Fe_2O_5$ along the $[10\bar{2}]_m$ zone axis.

$$\begin{bmatrix} a \\ b \\ c \end{bmatrix}^*_m = \begin{bmatrix} 1/7 & 1/\bar{7} & 1/\bar{7} \\ 0 & 1/4 & \bar{1}/4 \\ 2/14 & 1/14 & 1/14 \end{bmatrix} \begin{bmatrix} a \\ b \\ c \end{bmatrix}^*_c . \quad (1)$$

As a consequence the relationship between both direct cells is

$$\begin{bmatrix} a \\ b \\ c \end{bmatrix}_m = \begin{bmatrix} 1 & \bar{1} & \bar{1} \\ 0 & 2 & \bar{2} \\ 4 & 3 & 3 \end{bmatrix} \begin{bmatrix} a \\ b \\ c \end{bmatrix}_c . \quad (2)$$

The value of the determinant of this matrix ($|M| = 28$) implies that the monoclinic cell contains 28 perovskite subcells. A representation of the real cells is given in Fig. 2.

In a second step the atomic positions have been determined assuming (i) that the structure of $Ba_2Fe_2O_5$ derives from a c.f.c. "AO_3" stacking, the atoms occupying the same positions as in the cubic perovskite.

(ii) that the oxygen vacancies are randomly distributed.

In such a way the atomic positions in the monoclinic cell ($[r_i]_m$) have been determined according to the following relation:

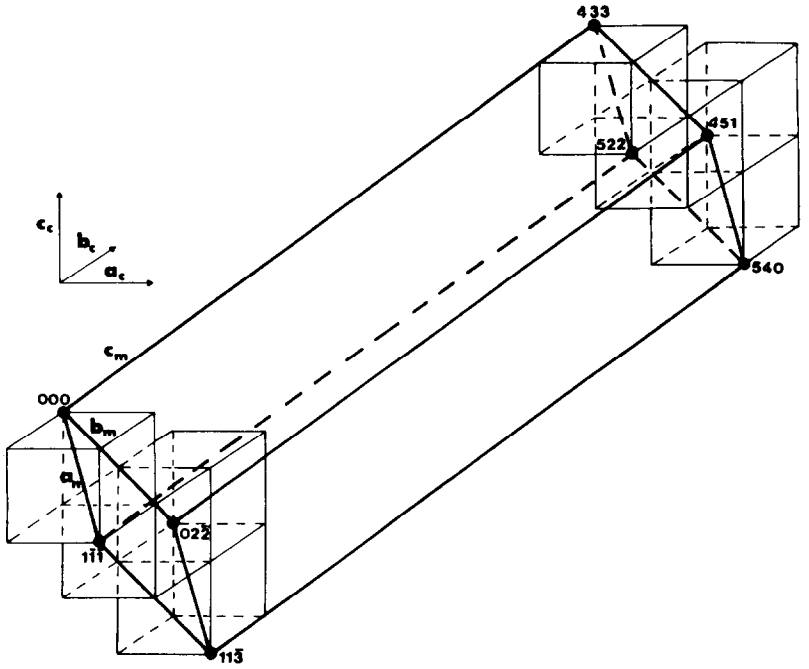

FIG. 2. Schematic representation of the real monoclinic and cubic cells.

—$[r_i]_m = M \cdot [r_i]_c$, $[r_i]_c$ being the atomic positions of Ba, Fe, and O in the cubic perovskite and M the matrix (1). This expression allowed us to locate the atoms in the monoclinic cell as follows:

7 (Ba), 7 (Fe), 20 (O) in the general position (*e*) with multiplicity 4,

1 (O) in the special position (*a*) with multiplicity 2,

1 (O) in the special position (*b*) with multiplicity 2.

On the basis of those assumptions, refining leads to some discrepancy between experimental and calculated X-ray diffractometers as a consequence of the hypothesis that the oxygen vacancies have not been located. However the refinement of the cell parameters and the assignment of the X-ray diffraction peaks could be satisfactorily carried out. In any case neutron diffraction experiments are highly necessary.

The refined cell parameters are a = 6.969(1) Å; b = 11.724(1) Å; c = 23.431(5) Å; α = 98.74(1)°. The final indexation is given in Table I.

Mössbauer Resonance Study

As the absorption of γ-rays is relatively high in barium compounds, $Ba_2Fe_2O_5$ has been doped with ^{57}Fe brought in during the preparation using 30% enriched α-Fe_2O_3.

The sample, sensitive to carbonatation as well as to hydrolysis, was shut up in an airtight cell schematically represented in Fig. 3 which allowed us to collect the Mössbauer data during several days. The material was placed between two pieces of aluminum foil covered with two mylar windows. The whole was pressed between two copper blocks constituting the sample holder.

The Mössbauer spectrum obtained at room temperature is reported in Fig. 4a. It characterizes a magnetically ordered phase but is much more complex (there are about

TABLE I

X-RAY DIFFRACTION DATA FOR $Ba_2Fe_2O_5$

d_{obsd}	$h\ k\ l$	I/I_{obsd}
10.43	0 0 1	4
4.136	1 2 $\bar{1}$	12
4.044	1 2 $\bar{3}$	24
3.860	0 3 $\bar{1}$	<1
3.666	0 1 $\bar{6}$	1
3.447	2 0 $\bar{2}$	3
3.304	2 1 $\bar{2}$	5
3.212	2 1 $\bar{3}$	6
3.175	2 0 2	1
3.170	1 0 6	1
3.058	1 1 6	3
3.028	1 3 3	3
2.933	0 4 0	52
2.907	2 2 $\bar{1}$	100
2.883	0 2 7	49
2.883	0 2 $\bar{7}$	49
2.791	2 0 $\bar{6}$	58
2.697	1 4 $\bar{1}$	2
2.693	1 4 $\bar{3}$	1
2.651	1 3 $\bar{6}$	3
2.531	2 1 7	3
2.461	1 3 6	10
2.391	1 4 $\bar{4}$	30
2.320	3 0 $\bar{2}$	14
2.298	1 0 $\bar{10}$	13
2.265	2 3 4	5
2.066	2 0 $\bar{8}$	35
2.020	2 4 6	64
2.001	3 1 $\bar{4}$	1
1.981	0 2 $\bar{11}$	3
1.938	2 4 7	2
1.846	3 2 $\bar{5}$	5
1.840	1 6 3	5
1.837	1 2 $\bar{11}$	5
1.821	3 4 2	5
1.812	0 4 $\bar{10}$	5
1.773	3 2 9	5
1.689	2 4 8	19
1.685	2 6 $\bar{1}$	17
1.682	0 6 7	10
1.682	0 6 $\bar{7}$	10
1.668	4 0 2	9

15 peaks) than those previously obtained for the homologous $Ca_2Fe_2O_5$ and $Sr_2Fe_2O_5$ phases of brownmillerite-type structure (Figs. 4b and 4c) (*12, 13*). This spectrum required relatively long recording times, but finally appears better resolved than those published by previous authors (*14, 15*).

Taking account of the complexity of the pattern—i.e., the presence of several sextuplets—the refinement was performed following several steps:

Mathematical refining. Assuming Lorentzian lines with a half-width $\Gamma = 0.28$ mm $\cdot$ s^{-1}, this refinement led to the determination of five sextuplets. The positions of the lines show the presence of Fe^{3+} in both octahedral and tetrahedral sites (as expected with respect to the homologous phases) but furthermore in an additional site (see arrowin Fig. 4a) with a chemical shift intermediate between the previous ones.

Refining of the Mössbauer parameters. In a second step a refinement was carried out assuming a hyperfine field distribution. The reliability factor obtained for each sextuplet is relatively low with a "misfit factor" ca. 1.7%, leading to the conclusion of the presence of discrete sites, well-defined from a crystallographic viewpoint.

The final results of the refinement are reported in Table II.

Based on the values of the isomer shifts and of the hyperfine fields, the following assignments have been proposed: three octahedral sites, one tetrahedral site, and one site with likely fivefold coordination with regard to the values of δ and H which are in agreement with previously observed values for Fe^{3+} in such a site (*16*).

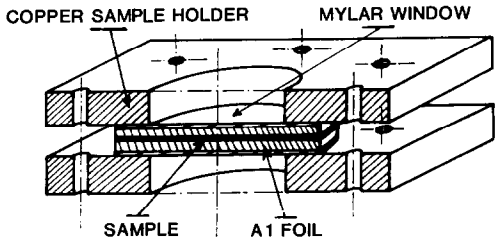

FIG. 3. Schematic representation of the Mössbauer resonance sample holder.

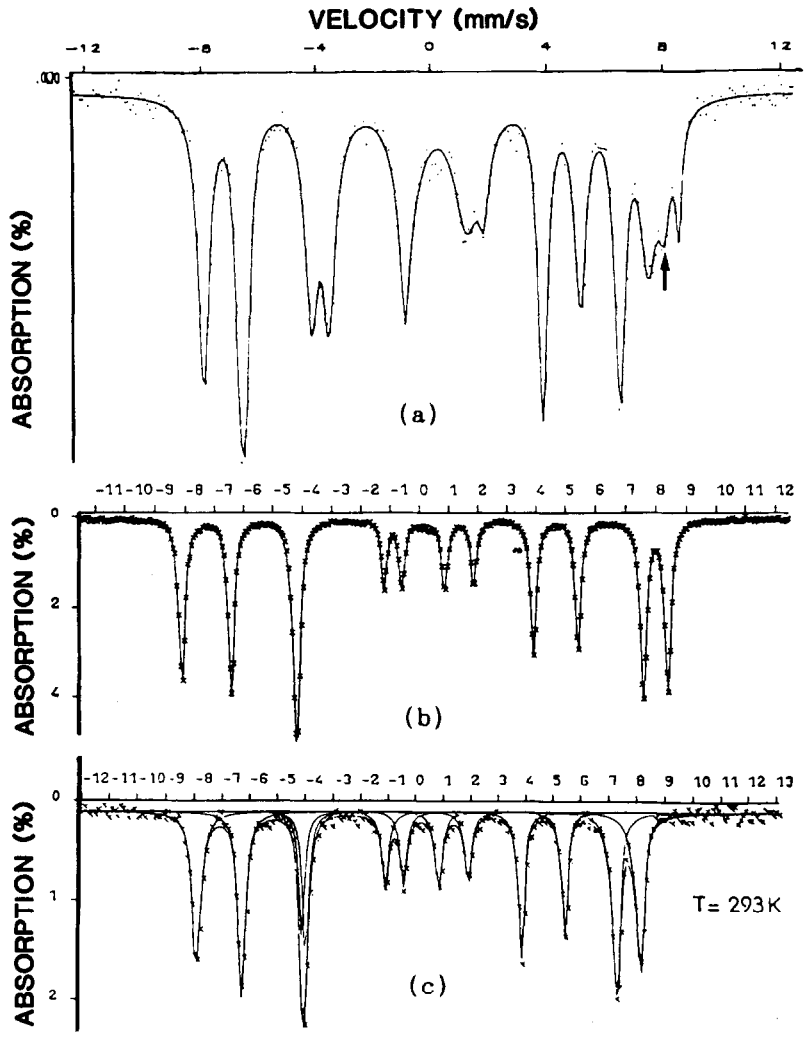

FIG. 4. Mössbauer resonance spectra at room temperature for (a) $Ba_2Fe_2O_5$, (b) $Ca_2Fe_2O_5$, and (c) $Sr_2Fe_2O_5$.

TABLE II

MÖSSBAUER PARAMETERS OF $Ba_2Fe_2O_5$ AT 293 K

Site	δ (mm · sec^{-1})	H (T)	ε (mm · sec^{-1})	A (%)
Octahedral 1	0.46	50.8	−0.07	14
Octahedral 2	0.45	49.5	−0.25	15
Octahedral 3	0.44	47.2	−0.41	14
Tetrahedral	0.15	40.4	−0.07	42
Fivefold	0.23	42.9	0.32	15

Note. δ, isomer shift; H, hyperfine field; ε, parameter directly related to the quadrupole splitting; A, Fe atomic percentage in a given site assuming identical recoilless fractions.

In addition the relative area of the peaks shows the sites to appear with following proportions:

$-O_h$	$1/7 + 1/7 + 1/7 = 3/7$
$-T_d$	$3/7$
—fivefold	$1/7$

Such a distribution supposes the existence of seven (or of a multiple of seven) iron atoms within the cell. This feature nicely agrees with the observed crystallographic cell which contains 28 Fe atoms. It seems

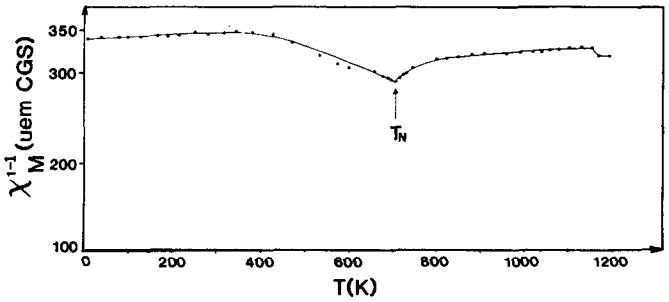

FIG. 5. Thermal evolution of the reciprocal magnetic susceptibility of $Ba_2Fe_2O_5$.

that only one tetrahedral site (T_d) exists whereas three octahedral ones (O_h) have been observed. The difference found for the Mössbauer parameters is probably due to the existence of variable cationic environments. Taking into account both the oxygen stoichiometry (i.e., 1/6 oxygen vacancy per motive) and the equal number of O_h and T_d sites, one may conclude that the last site is necessarily fivefold coordinated leading to the developed formula:

$$Ba_{28}[FeO_3]_{12}[FeO_2]_{12}[FeO_{2.5}]_4O_{70} \equiv Ba_{28}Fe_{28}O_{70} \equiv Ba_2Fe_2O_5.$$

Magnetic and Electrical Properties

The magnetic behavior of $Ba_2Fe_2O_5$ has been investigated using a Foner magnetometer and a Faraday-type magnetic balance. The thermal variation of the reciprocal molar susceptibility is reported in Fig. 5. It characterizes an antiferromagnetic compound whose Néel temperature is close to 720 K. Such a rather high ordering temperature value involves the existence of strong magnetic couplings. Below T_N no ferromagnetic component has been observed. The paramagnetic domain shows an anomalous variation of the magnetic susceptibility. The experimental C_M and consequently θ_P constants are much larger (and even meaningless) than the theoretical values expected for 2 Fe^{3+} ($3d^5$; $C_M \simeq 8.75$) and even than the values previously observed for the homologous compounds $A_2Fe_2O_5$ (A = Ca, Sr) (Table III). This phenomenon has been explained for these compounds in terms of thermal variation of the molecular field constants related to the existence of strong magnetic interactions (*17*). However, it should be pointed out that $Ba_2Fe_2O_5$ behaves somewhat differently and one cannot compare them carefully as the crystal and magnetic structures of $Ba_2Fe_2O_5$ are still unknown.

In addition, at 880°C ($\simeq$ 1150 K), a magnetic transition, corresponding to a slight increase of the susceptibility, is observed. It is related to a structural monoclinic $\Leftrightarrow$ cubic transition identified by X-ray diffraction and D.T.A. It is likely similar to the transition already observed in $Sr_2Fe_2O_5$ (*18*).

The electrical conductivity has been measured using the four probe method on a pelleted sample between 250 and 500 K. The thermal evolution (Fig. 6) reveals a semicon-

TABLE III

MAGNETIC DATA OF THE $A_2Fe_2O_5$ (A = Ca, Sr, Ba) PHASES

Material	T_N (K)	C_M (uem) CGS	θ_P (K)
$Ca_2Fe_2O_5$	725	14.50	−3100
$Sr_2Fe_2O_5$	715	13.35	−2840
$Ba_2Fe_2O_5$	720	(24.8)	(−7075)

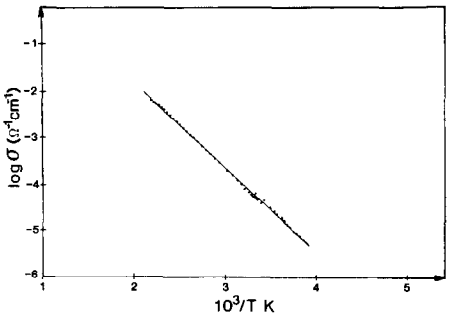

FIG. 6. Evolution of the logarithm of electrical conductivity of $Ba_2Fe_2O_5$ with reciprocal temperature.

ducting behavior with an activation energy relatively high (ΔE = 0.35 eV) characterizing a strong electronic localization.

Conclusion

Both crystallographic results and Mössbauer resonance study obviously show that $Ba_2Fe_2O_5$ differs significantly from $Ca_2Fe_2O_5$ or $Sr_2Fe_2O_5$. However, it is worthwhile to notice that the high value of T_N, close to those observed for the homologous compounds (Table III), implies that the magnetic interactions are of the same order of magnitude, i.e., as expected from superexchange-type 180° Fe^{3+}–O–Fe^{3+} interactions. Therefore, as previously suggested from the X-ray diffraction investigation of the $BaFeO_{3-y}$ system, this result supposes that the structure of $Ba_2Fe_2O_5$ derives from a cubic "BaO_3" stacking. Indeed, had the structure been related to a hexagonal stacking, the interactions would proceed through common faces (or edges due to presence of vacancies) and consequently would be weaker leading to a lower Néel temperature.

Unlike the results concerning homologous calcium and strontium ferrites and previous data relative to $Ba_2Fe_2O_5$, our Mössbauer study shows the presence of an additional fivefold coordinated site. From a crystallographic point of view, as previously described by S. Komornicki *et al.* (*19*), the existence of tetrahedral sites in perovskite-related ferrites implies vacancy ordering along rows (as in $Ca_2Fe_2O_5$ and $Sr_2Fe_2O_5$) whereas the formation of fivefold coordinated sites requires isolated oxygen vacancies. Consequently we can conclude that the vacancy ordering in $Ba_2Fe_2O_5$ is certainly different from that observed in the brownmillerite compounds, resulting in a complex monoclinic unit cell.

Comparative Mössbauer resonance data are given in Table IV. It should be pointed out that the values of the hyperfine fields for the O_h and T_d sites are similar in the three phases in agreement with close Néel temperatures. But the isomer shifts (δ) markedly differ; the δ_{O_h} value is higher in $Ba_2Fe_2O_5$ which could be attributed to less covalent (i.e., longer) $(Fe–O)_{O_h}$ bonds probably as a consequence of a dilatation effect resulting from the big size of barium. Re-

TABLE IV

MÖSSBAUER RESONANCE PARAMETERS AT 293 K FOR $Ca_2Fe_2O_5$, $Sr_2Fe_2O_5$, AND $Ba_2Fe_2O_5$

	δ_{O_h} (mm · sec^{-1})	H_O (T)	A (%)	δ_{T_d} (mm · sec^{-1})	H_{O_h} (T)	A (%)	$\delta_{fivefold}$ (mm · sec^{-1})	$H_{fivefold}$ (T)	A (%)
$Ca_2Fe_2O_5$	0.37	50.9	49	0.21	42.9	51			
$Sr_2Fe_2O_5$	0.36	43.5	47	0.21	40.3	53			
	0.44	47.2							
$Ba_2Fe_2O_5$	0.45	49.5	43	0.15	40.4	42	0.23	42.3	15
	0.46	50.8							

versely the lower δ_{T_d} value would correspond as a counterpart to an enhanced covalency of the tetrahedral sites. But such conclusions should be ascertained by careful structural determination.

References

1. J. C. GRENIER, A. WATTIAUX, M. POUCHARD, P. HAGENMULLER, M. PARRAS, M. VALLET, J. M. GONZALEZ-CALBET, AND M. ALARIO, *J. Solid State Chem.* **80,** 6 (1989).
2. J. GONZALEZ-CALBET, M. PARRAS, M. VALLET-REGI, AND J. C. GRENIER, *J. Solid State Chem.*, submitted for publication.
3. M. PARRAS, M. VALLET, J. M. GONZALEZ, M. A. ALARIO-FRANCO, J. C. GRENIER, AND P. HAGENMULLER, *Mater. Res. Bull.* **22,** 1413 (1987).
4. E. F. BERTAUT, P. BLUM, AND A. SAGNIÉRES, *Acta Crystallogr.* **12,** 149 (1959).
6. P. K. GALLAGHER, J. B. MACHESNEY, AND D. N. E. BUCHANAN, *J. Chem. Phys.* **42(2),** 516 (1965).
7. S. MORI, *J. Amer. Ceram. Soc.* **49(11),** 600 (1966).
8. M. ZANNE, Thesis, Université de Nancy (1972).
9. E. LUCCINI, S. MERIANI, AND D. MINICELLI, *Acta Crystallogr., Sect. B* **29,** 1217 (1973).
10. J. GONZALEZ-CALBET, M. PARRAS, M. VALLET-REGI, AND J. C. GRENIER, *J. Solid State Chem.* in press (1989).
11. "International Tables for Crystallography," Vol. A, Kluwer Academic, Norwell, MA (1987).
12. J. C. GRENIER, L. FOURNÉS, M. POUCHARD, P. HAGENMULLER, AND S. KOMORNICKI, *Mater. Res. Bull.* **17,** 55 (1982).
13. L. FOURNÉS, Y. POTIN, J. C. GRENIER, AND P. HAGENMULLER, *Rev. Phys. Appl.* **24,** 463 (1989).
14. T. ICHIDA, Y. BANDO, AND T. SHINJO, *Bull. Inst. Chem. Res., Kyoto Univ.* **51(5)** (1973).
15. J. B. MACCHESNEY, P. K. GALLAGHER, AND D. N. E. BUCHANAN, *J. Chem. Phys.* **43,** 516 (1965).
16. F. MÉNIL, *J. Phys. Chem. Solids* **46(7),** 763 (1985).
17. J-C. GRENIER, M. POUCHARD, AND R. GEORGES, *Mater. Res. Bull.* **8,** 1413 (1973).
18. J-C. GRENIER, N. EA, M. POUCHARD, AND P. HAGENMULLER, *J. Solid State Chem.* **58,** 243 (1985).
19. S. KOMORNICKI, J-C. GRENIER, M. POUCHARD, AND P. HAGENMULLER, *Nouv. J. Chim.* **5,** 161 (1981).